Atmospheric Environment Vol. 25B, No. 3, pp. 311–326, 1991.
Printed in Great Britain.

0957–1272/91 $3.00+0.00

AN OBJECTIVE URBAN HEAT STORAGE MODEL AND ITS COMPARISON WITH OTHER SCHEMES

C. S. B. GRIMMOND,* H. A. CLEUGH† and T. R. OKE‡

*Climate and Meteorology Program, Department of Geography, Indiana University, Bloomington, IN 47405, U.S.A., †School of Earth Sciences, Macquarie University, North Ryde NSW 2109, Australia and ‡Atmospheric Science Programme, Geography Department, University of British Columbia, Vancouver, BC, Canada, V6T 1W5

(*First received* 5 *November* 1990 *and in final form* 18 *May* 1991)

Abstract—An objective hysteresis model to predict the storage heat flux in urban areas is presented. A review of observational and theoretical work reveals this approach to be more appropriate than the linear relation between soil heat flux and net all-wave radiation. A scheme to implement the model in any urban area is developed. In essence the model only requires land cover and net all-wave radiation as input, but it can be further refined to include anthropogenic heat release, the three-dimensional form of the surface, and can allow for changes in source area. Tests against energy balance data from a site in Vancouver, BC indicate the model simulates most aspects of measured storage heat flux values for a suburban site in both winter and summer. Comparison with the results of a study in Bonn, Germany involving the use of heat flux plates and detailed heat content change calculations gives good agreement except for a phase difference of about 1 h. There is evidence to suggest that the spatial variation of intra-urban heat storage may be relatively conservative.

Key word index: Urban heat storage, urban climate models, energy balance.

1. INTRODUCTION

In urban areas, the sub-surface or storage heat flux (ΔQ_S) is the net uptake or release of energy from the urban system. It includes latent and sensible heat changes in the air, buildings, vegetation, and ground extending from above roof-level to a depth in the ground where net heat exchange over the period of study is negligible (Oke and Cleugh, 1987). A knowledge of this term and an ability to determine its magnitude in the energy balance is important in urban climatology. It is often needed as part of methods to evaluate evaporation (e.g. Grimmond *et al.*, 1986) and the thermal inertia provided by storage is often regarded as a key term in the genesis of the urban heat island (Goward, 1981).

It is relatively easy to obtain a value for the soil heat flux where the surface is well defined and homogeneous at the spatial scale of interest. In urban environments, however, the active surface is both multifaceted and extremely complex. To help overcome this, the concept of a surface volume is adopted. We set the top of the volume to just above roof/tree level and the base to a depth in the ground where no net vertical heat transport takes place over the period of interest. Then the 'storage heat flux' (ΔQ_S) is defined to include the conduction of heat into or out of the surface media comprising the volume (e.g. walls, roofs, trees, ground, etc.), and changes in the sensible and latent heat content of the air volume itself. A similar approach is taken to the storage heat flux in forested canopies (see Aston, 1985; Moore and Fisch, 1986). In the case of forests it is feasible to replicate temperature sensors for each canopy component and to use them together with an estimate of biomass and the heat capacity of wood to calculate the storage change. But, when dealing with the much greater diversity of cities, this approach requires such a multiplicity of sensors to adequately sample the system that it is only possible as a short-term undertaking (Peikorz, 1987; Kerschgens and Kraus, 1990).

If all other terms of the surface energy balance are independently evaluated ΔQ_S can be found as the residual:

$$\Delta Q_S = Q^* + Q_F - Q_H - Q_E \quad (1)$$

where Q^* is the net all-wave radiation flux density; Q_F the anthropogenic heat flux density (note herein the sum $Q^* + Q_F$ is given the separate symbol Q^+); and Q_H, Q_E the turbulent sensible and latent heat flux densities, respectively. Heat storage values determined by residual (ΔQ_{SR}) will be used here to provide test data but such data are not routinely available.

There is a need to develop a simple way to obtain the heat storage in urban systems. One approach is to examine heat flow into materials such as grass, concrete or other urban materials and use these as a surrogate for urban behavior. Kerschgens and Hacker (1985) and Kerschgens and Drauschke (1986) use measurements of the substrate heat flux into grassed and paved sites and combine them into an urban system estimate by weighting the results according to the fraction of green and impervious cover in the upwind region.

Another approach, and that adopted herein, is to parameterize heat storage change in terms of the net

all-wave radiation which forces the energetics of the system. The equation is essentially empirical but its form has both theoretical and physical support. The present scheme includes an objective method to characterize the urban surface, hence it can be applied more generally to other urban areas.

This paper gives the rationale for the form of an equation proposed, outlines the way in which coefficients are developed and the scheme is applied to a given city, and tests the model against 'measured' data obtained by residual from energy balance observations at a suburban site. The model is also compared with other schemes.

2. PARAMETERIZATION OF SUBSTRATE HEAT FLUXES

In many mesoscale and even global climate models the proportion of the surface energy input which is used to heat the substrate materials is set to a simple fraction of the surface net all-wave radiation, i.e. $Q_G = aQ^*$. The first attempt to parameterize heat storage change in cities used a similar approach but incorporated an offset (Oke *et al.*, 1981). It took published relations of this form for several urban surface materials and combined them in a composite equation which weighted the role of each according to their plan coverage in the area under study, so that:

$$\Delta Q_S = \sum_{i=1}^{n} \alpha_i (a_i Q^* + b_i) \qquad (2)$$

where α_i is the fraction of the urban area covered by the ith surface. The general performance of this objective linear model was satisfactory especially when used for periods of a day or more. However, it was unable to provide accurate hourly values at all times of the day because the linear form of the model could not allow it to match observed phase shifts between ΔQ_S and Q^*. These characteristics were confirmed by a more rigorous test (Oke and Cleugh, 1987).

Several observational studies of homogeneous surfaces have investigated the relation between Q^* and Q_G (e.g. Sellers, 1965; Monteith, 1973; Clothier *et al.*, 1986). Although most assume *a priori* that this relation is linear, their results show it to be non-linear giving a hysteresis loop if Q_G is plotted as a dependent variable of Q^* (Fig. 1). Similar examples are given by Fuchs and Hadas (1972), Idso *et al.* (1975), Camuffo and Bernardi (1982) and de Bruin and Holtslag (1982). Lettau (1951) presents a theoretical model for surface temperature, assuming that the radiant energy at a bare soil surface can be described as a harmonic function, and using a prescribed, constant evaporation rate. He derives an analytic solution showing that the diurnal pattern of the soil heat flux precedes that of the surface temperature by 3 h and the net all-wave radiation by about half that interval. Camuffo and Bernardi (1982) proposed the following form of equation which explicitly

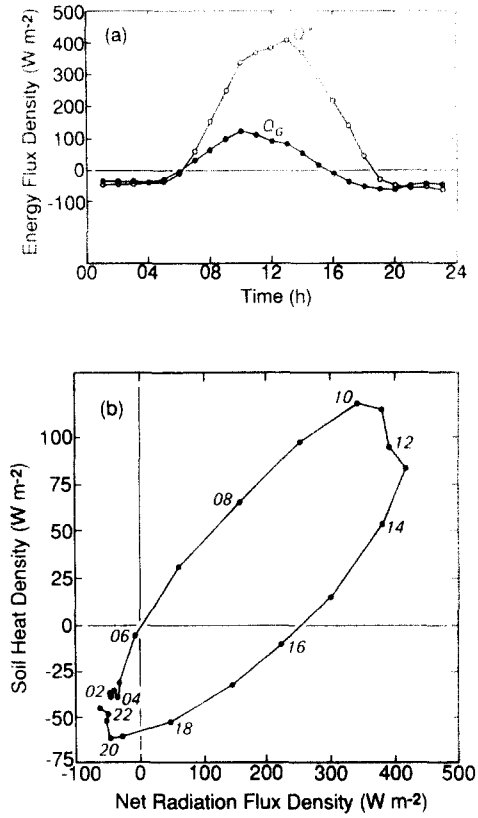

Fig. 1. (a) Time series and (b) hysteresis loop relations between soil heat flux and net all-wave radiation for short grass near St Louis, MO calculated from the data of Doll *et al.* (1985) for a single day. Best fit statistics give the equation: $Q_G = 0.32Q^* + 0.54(\partial Q^*/\partial t) - 27.4$.

recognizes this:

$$\Delta Q_S = a_1 Q^* + a_2 \frac{\partial Q^*}{\partial t} + a_3 \qquad (3)$$

where t is time. Thus, the soil heat flux density is expressed both as a function of net all-wave radiation and the rate and direction of change of radiant forcing. The a_1 and a_3 coefficients perform the same role as a and b in Equation (2), but a_2 accounts for hysteresis. A positive value implies a peak in the soil heat flux prior to a peak in the net all-wave radiation.

While Lettau's analytic solution provides some theoretical explanation for the observations of an out-of-phase relation, a physical explanation for the hysteresis loop is difficult to find in the literature. Of course the ratio of the atmospheric and soil thermal admittances and its variation through a day influences the Q_G/Q^* partitioning. In the morning hours, the atmosphere is relatively stable and the mixed layer is confined to a shallow layer before the nocturnal inversion is completely eroded. Hence sensible heat is transferred more readily into the soil. In the afternoon when the atmosphere is unstable, and the coupling of the boundary and surface layers is greatest, the turbu-

lent transfer of heat into the atmosphere is vastly more efficient than conduction into the soil.

Oke and Cleugh (1987) showed that the form of Equation (3) was appropriate to the case of heat storage in the city. A good statistical fit to their small data set from a suburban site in Vancouver, BC was obtained with $a_1 = 0.35$, $a_2 = 0.28$ h and $a_3 = -40$ W m^{-2}, with fluxes in units of W m^{-2}. However, it should be noted that this is purely empirical and holds no inherent predictive power elsewhere or at other times.

3. AN OBJECTIVE HYSTERESIS STORAGE HEAT FLUX MODEL

Given the appropriateness of the form of Equation (3) and the great merits of objectivity and simplicity of Equation (2) the two are combined to produce an objective scheme capable of incorporating hysteresis.

The approach adopted consists of three parts. First, the area under study is surveyed to create an inventory of the building dimensions, the distribution of surface materials and information necessary to characterize the study area and to calculate the size of the anthropogenic heat release from the area (section 3.1). Second, independent data sets involving simultaneous measurements of net all-wave radiation and substrate heat flux density for the range of urban surface materials are selected and statistically analysed to obtain the coefficients a_1–a_3 (section 3.2). Third, the contribution made by the coefficients from each surface derived in the second part are weighted by the results in the first part to give an equation which is unique to this site of the form:

$$\Delta Q_S = \sum_{i=1}^{n} \{a_{1i} Q^* + a_{2i}(\partial Q^*/\partial t) + a_{3i}\} \qquad (4)$$

where, when $\Delta t = 1$, $\partial Q^*/\partial t = 0.5(Q^*_{t+1} - Q^*_{t-1})$. $\partial Q^*/\partial t$ has units of W m^{-2} h^{-1}; and the coefficients a_1, a_2, and a_3 are dimensionless, h, and W m^{-2}, respectively. Our experience shows that, while Equation (4) is appropriate to the daytime, a different partitioning occurs at night. At that time the turbulent terms in Equation (1) are usually small but Q_F can become a significant fraction of the available energy, so that the approximation $\Delta Q_S = Q^+$ is often a good representation. Accordingly this equality is used when Q^+ is negative. The storage flux parameterized using this objective hysteresis model (OHM) is that for a spatially integrated surface ranging in scale from a city block (approximately 0.5×0.5 km) to an urban land-use zone.

3.1. *Surface survey*

Following Oke *et al.* (1981), the area under study is divided into the following basic surface cover types which characterize most urban areas:

(a) greenspace/open—both unirrigated and irrigated; and

(b) built—horizontal, paved areas (concrete, asphalt, etc.), rooftops, and canyon structures (i.e. street and flanking building sides).

The relative proportion of each of these components is calculated from data gathered by a surface cover survey. In order to take account of the three-dimensional nature of the suburban environment, the full surface area in contact with the atmosphere, the active surface area, is calculated. For example, a building has at least four wall areas and a roof, not just its plan area, involved in heat uptake and loss. This is an improvement over the scheme used by Oke *et al.* (1981). Obviously in areas of high building density, especially multi-storey structures, the new weighting allows for an appropriate emphasis to be given to the walls, since the active surface area will be much greater than the plan area. In the low density suburban area of Vancouver reported here the active: plan ratio is about 1.5.

The three-dimensional form of large vegetation elements is not accounted for in OHM. There are no data pertinent for heat storage by single trees or bushes but after considering the storage in the biomass of forests (Aston (1985)—young eucalyptus: $a_1 = 0.0004$, $a_2 = 0.18$ h, $a_3 = 3.9$ W m^{-2}; McCaughey (1985)—mixed forest: $a_1 = 0.11$, $a_2 = 0.11$ h and $a_3 = -12.3$ W m^{-2}) we consider it probably to be too small to include.

When trying to characterize the role of heat storage in the energy balance of areas where surface characteristics (cover types and building density) do not exhibit marked spatial inhomogeneity it is sufficient to use an areal average of the surface properties centered on the site of interest. However, in more heterogeneous areas, the properties of the source areas of the measured fluxes (such as Q^*, Q_H and Q_E) must be correctly matched with those of calculated fluxes (such as Q_F and ΔQ_S) to produce a spatially consistent energy balance. Here we use a 'dynamic' scheme to identify rationally the correct source area for Q_F and ΔQ_S.

The fluxes measured at a point are influenced by the surface types present in the surrounding area. That is, although one is measuring at a point, the fluxes that are measured are representative of an area. The location and shape of the area that influences measured fluxes depends both on the flux sensing system and the meteorological conditions. Given the relative conservativeness in the spatial variability of net all-wave radiation, Schmid *et al.* (1991) propose that the area for surface description should correspond to the source area of the turbulent fluxes. This area is upwind of the measurement location and aligned along the prevailing wind direction. The upwind, downwind and lateral boundaries of the source area depend on the characteristics of the flow and on the boundary layer development in the atmospheric layer between the surface and the sensor. The boundaries of this area (A_{pl}) are determined using the plume Source Area Model (SAM) described by Schmid and Oke (1990).

The model requires values of the site roughness and zero-plane displacement, Obukhov stability length, friction velocity, standard deviation of wind direction and mean wind speed as input. A simplified method for determining this area using source area sectors (A_{se}) rather than plume areas is also used (for a full explanation see Schmid *et al.*, 1991). The source area (A_{pl} or A_{se}) calculated for any given hour is overlain on a database composed of 100×100 m grid squares containing information about the surface (building type, number and area; vegetation and area, road type and area, population, etc.).

3.2. *Equation coefficients*

Within the surface cover categories outlined it is appropriate to incorporate surfaces of special importance in a given city if a data set relating ΔQ_S to Q^* is available for analysis. The following are the relations we use for a mid-latitude city. As more and better data sets become available they should be used to update and modify these coefficients.

Greenspace/open. The three data sets used (Table 1a) all include the effects of storage changes between the surface and the depth of the heat flux plate. The grass sets refer to short grass typical of urban lawns. In order to include the effects of irrigation both moist (Doll *et al.*, 1985) and dry (Clarke *et al.*, 1971) conditions were included. The distinction did not seem very significant so both sets, in addition to a bare soil set, were aggregated together with equal weighting. This may be inappropriate at sites where irrigation/grass is dominant or absent. An example of the type of ΔQ_S vs Q^* hysteresis loop relations obtained using grass data is given in Fig. 1.

Roofs. Two sets for large buildings were used (Table 1a). In view of the disturbingly large difference between the two it would be very helpful to have a wider range of roof types included in the set.

Paved. Two sets of data, one for concrete and one for asphalt (Table 1a), were aggregated together with equal weight given to each.

Canyon. Results from a north–south oriented canyon in Vancouver, BC are used (Table 1a). The a_2 coefficient in this relation is relatively small. In more detail the results presented in Fig. 2 show that there is a significant hysteresis loop associated with each of the canyon facets (east and west walls and the floor) but they are both short-lived and occur at very different times due to the irradiance pattern for the facets. The direction of the loop also varies between facets. The

Table 1. Summary of equations used in parameterization scheme

(a) *Development coefficients for OHM*

Land cover	Author	Regression coefficients a_1	a_2 (h)	a_3 (W m^{-2})
1. Greenspace/Open				
Short grass	Doll *et al.* (1985)	0.32	0.54	−27.4
Grassland	Clarke *et al.* (1971)	0.33	0.03	−11.0
Bare soil	Novak (1981)	0.38	0.56	−27.3
2. Rooftop				
Vancouver	Yap (1973)	0.17	0.10	−17.0
Uppsala	Taesler (1980)	0.44	0.57	−28.9
3. Paved				
Concrete	Doll *et al.* (1985)	0.81	0.48	−79.9
Asphalt	Narita *et al.* (1984)	0.36	0.23	−19.3
4. Canyon				
N–S canyon	Nunez (1974)	0.32	0.01	−27.7

(b) *Example of coefficient calculation*

Land cover	Weighting factor			
Greenspace/open	0.43	0.145	0.161	−11.8
Rooftop	0.13	0.039	0.044	−2.98
Paved	0.11	0.064	0.039	−5.46
Canyon	0.33	0.106	0.005	−9.14
Model coefficients		0.35	0.25	−29.4

(c) *OHM coefficients for Sunset*

Surface information	Area				Period
Aerial photograph	2 km circle	0.35	0.25	−29.4	
Surface database	2 km circle	0.38	0.27	−29.3	
Surface database	A_{pl}	0.37	0.27	−29.1	All hours*
Surface database	A_{se}	0.37	0.27	−29.1	All hours*
Surface database	A_{pl}	0.37	0.27	−29.4	$Q^+ > 0$*
Surface database	A_{se}	0.37	0.26	−29.2	$Q^+ > 0$*

* Mean coefficients for hours when 1987 ΔQ_{SR} available.

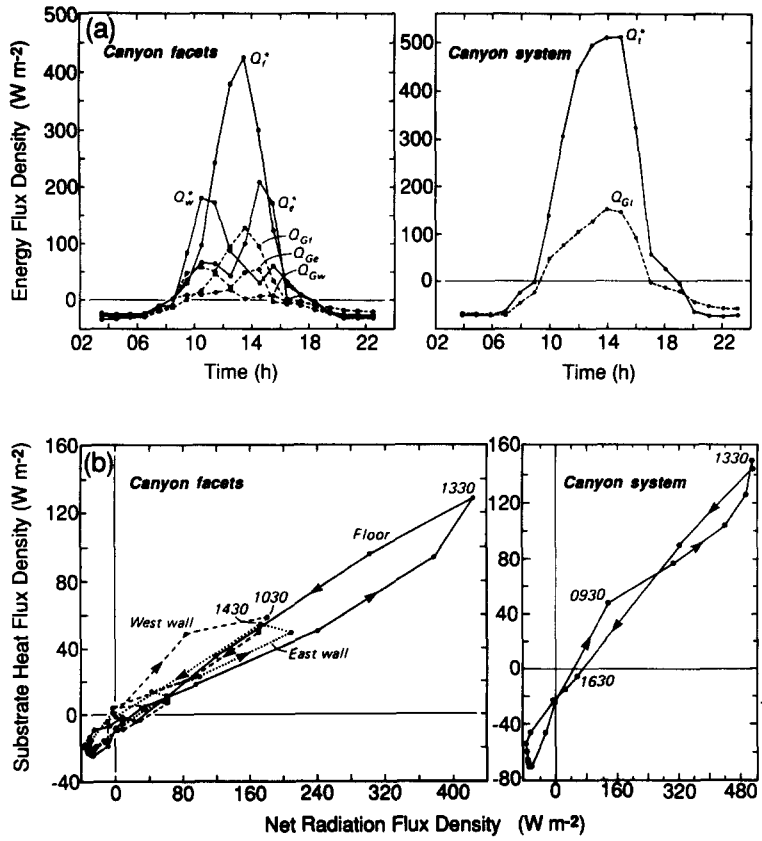

Fig. 2. (a) Time series and (b) hysteresis loop relations between substrate heat flux density and net all-wave radiation for a north–south oriented canyon including both individual canyon facets and the total canyon system. From a study by S. Ferguson (pers. comm., 1987) using the measurements of Nunez (1974) for 10 August 1973. Canyon system averages of Q^* and Q_G are calculated as an equivalent flux through the canyon top, e.g. $Q_t^* = Q_f^* + (H/W)(Q_e^* + Q_w^*)$ where the subscripts t,w,e and f stand for top, west wall, east wall and floor, respectively, and H and W are the canyon height and width.

net result of these complexities tend to offset each other so that the canyon system response is muted and surprisingly smooth with little evidence of hysteresis. The same may not be the case for an east–west oriented canyon where the Equator-facing wall rather than the floor will be the most energetically active facet.

3.3. *Equation weighting*

In the example given in Table 1b each surface relation inside a surface cover category is given equal weight. If very detailed site survey results are available (e.g. if the areal coverage of concrete and asphalt is known precisely) rational weighting within these categories can be conducted before the individual equations are weighted according to active area.

4. IMPLEMENTATION AND TEST OF OHM

The objective hysteresis model is applied to the same suburban site used by Oke *et al.* (1981) and Oke and Cleugh (1987) and tested using energy balance measurements from a micrometeorological tower for two periods, April–October 1986 and January–June 1987.

4.1. *Site survey and weighting*

The tower is located in a suburban neighborhood called Sunset in Vancouver, BC. The land-use is relatively homogeneous consisting primarily of single family residences with an average building height of about 8.5 m. Two methods are used to determine the necessary surface information: aerial photographs (Cleugh, 1990); and a surface database developed from city land-use maps and field surveys (Grimmond, 1988, 1992).

A survey of the aerial photographs shows 23,381 buildings in a 2 km radius circle centered on the tower of which 64% are houses, 34% garages and 2% are larger commercial or institutional buildings. There are about 1.8 buildings per 1000 m^2 of plan area and these have a mean wall area of 279 m^2. The average 1000 m^2 lot area contains approximately 500 m^2 of wall area,

200 m^2 of roof, 640 m^2 of greenspace and about 160 m^2 of paved area. This gives a total active area of 1500 m^2 for each 1000 m^2 of plan area. From the foregoing it follows that about 43% of the active area is greenspace, 13% is roof, 11% is paved and 33% is walls (or canyon). These are the weighting factors applied to the surface cover categories to arrive at the final coefficients for the aerial photographs reported in Table 1b, viz. $a_1 = 0.35$, $a_2 = 0.25$ and $a_3 = -29.4$.

The surface database contains information for 100 × 100 m cells for a 5 km radius circle centered on the tower. This was used to determine the weighted coefficients for a 2 km radius circle and to determine the coefficients for the source area for each hour as outlined in section 3.1. Table 1c reports the mean coefficients for the study period.

4.2. *Micrometeorological data*

The estimates of urban heat storage change using the model are compared against those obtained as a residual using Equation (1). Q^* for both methods was measured by a net pyrradiometer (Swissteco, Model S1) mounted at a height above ground of 29 m (an effective height of about 20 m after allowance for terrain and roughness features). Given the small spatial variability of net all-wave radiation at this site (Schmid *et al.*, 1991) a point measurement is deemed sufficient. Q_F was calculated following a procedure based on the work of Bach (1970) (see Grimmond, 1988, 1992 for details). It includes heat released from mobile and fixed combustion sources and the metabolism of humans and animals. Eddy correlation measurements of the turbulent heat flux density (Q_H) were obtained at the same height as the Q^* measurements using a sonic anemometer–thermometer system (Campbell Scientific, Model CA27) which sampled temperature and vertical velocity at 10 Hz. A reversing differential psychrometer, similar to that of McCaughey *et al.* (1987), operating over a height interval of 7.2 m with the top level at 29 m, was used to determine the Bowen ratio ($\beta = Q_H/Q_E$). Hence the storage heat flux residual (ΔQ_{SR}) was obtained as:

$$\Delta Q_{SR} = Q^* - Q_H - Q_H/\beta. \quad (5)$$

Oke and Cleugh (1987) note that the method is open to inaccuracies due to the accumulation of errors in the residual term. Their error analysis is applicable to the present study. Thus we anticipate maximum probable errors in measured ΔQ_S of about 50% ($\approx 14\%$ of Q^*) by day and about 25% ($\approx 18\%$ of Q^*) at night, but typical errors will be less. In 1987 there were 1586 h when all terms were available. Of these 23% had a potential error in β of $< 10\%$ and 37% had a potential error of $< 20\%$.

4.3. *Test results*

Table 2a gives the results of a statistical analysis comparing ΔQ_S calculated using OHM including the objective coefficients in Table 1c, against the corresponding 'measured' ΔQ_{SR} values (see section 4.2) when

Table 2. Statistical results for 1987 comparison between 'measured' and modelled ΔQ_s. The 'measured' ΔQ_s uses β values with errors of $\leqslant 20\%$

Surface method	Source area	m_f	r^2	RMSE (W m^{-2})	MAE (W m^{-2})	d	N&S	n
(a) *OHM*								
All hours								
Aerial photograph	2 km rad	0.76	0.87	30.7	21.7	0.95	0.84	595
Surface database	A_{pl}	0.83	0.87	36.8	25.1	0.96	0.86	285
Surface database	A_{sc}	0.81	0.87	29.3	20.5	0.95	0.85	595
Q^+ (positive)								
Aerial photograph	2 km rad	0.72	0.60	70.2	53.2	0.83	0.52	72
Surface database	A_{pl}	0.69	0.50	69.9	52.8	0.80	0.47	61
Surface database	A_{sc}	0.77	0.59	66.8	50.3	0.56	0.56	72
All hours: if Q^+ negative ΔQ_s modeled $= Q^+$								
Aerial photograph	2 km rad	0.85	0.90	26.3	11.0	0.96	0.88	595
Surface database	2 km rad	0.90	0.90	25.2	10.8	0.97	0.89	595
Surface database	A_{pl}	0.85	0.89	35.4	25.1	0.96	0.87	285
Surface database	A_{sc}	0.85	0.90	26.4	11.1	0.96	0.88	595
All hours: if $Q^+ \leqslant 0$ ΔQ_s modeled $= 0.98Q^+ + 0.004\,\partial Q^+/\partial t + 2.5$								
Aerial photograph	2 km rad	0.83	0.90	26.0	10.9	0.96	0.88	595
Surface database	2 km rad	0.89	0.90	24.9	10.6	0.97	0.89	595
Surface database	A_{pl}	0.88	0.89	33.8	15.9	0.97	0.88	285
Surface database	A_{sc}	0.87	0.90	25.1	10.8	0.97	0.89	595
(b) *Linear model*								
All hours								
Aerial photograph	2 km rad	0.64	0.87	36.6	25.1	0.91	0.77	595
Q^+ (positive)								
Aerial photograph	2 km rad	0.54	0.48	88.0	66.8	0.69	0.25	72

the error in β was $\leqslant 20\%$. It should be noted that the data set is biased towards hours when Q^+ is negative. The measures of goodness of fit reported are the slope of the linear functional relation (m_f) between the residuals and the modelled flux (Mark and Church, 1977), the coefficient of determination (r^2), Willmott and Wicks' (1980) index of agreement (d), and Nash and Sutcliffe's (1970) 'goodness of fit' (N&S). The root mean square error (RMSE) and the mean absolute error (MAE) also are included.

The inclusion of a separate equation for the hours when Q^+ is negative leads to an even better performance of OHM (Table 2a, Figs 3a and 3b). The least satisfactory feature of the OHM is its apparent tendency to underestimate the largest ΔQ_S flux densities (Figs 3a –3c). There appears to be a 'capping' on the modeled ΔQ_S. The maximum 'measured' $\Delta Q_{SR} \approx 370$ W m^{-2}, whereas the maximum modeled $\Delta Q_S \approx 290$ W m^{-2} (Fig.3b).

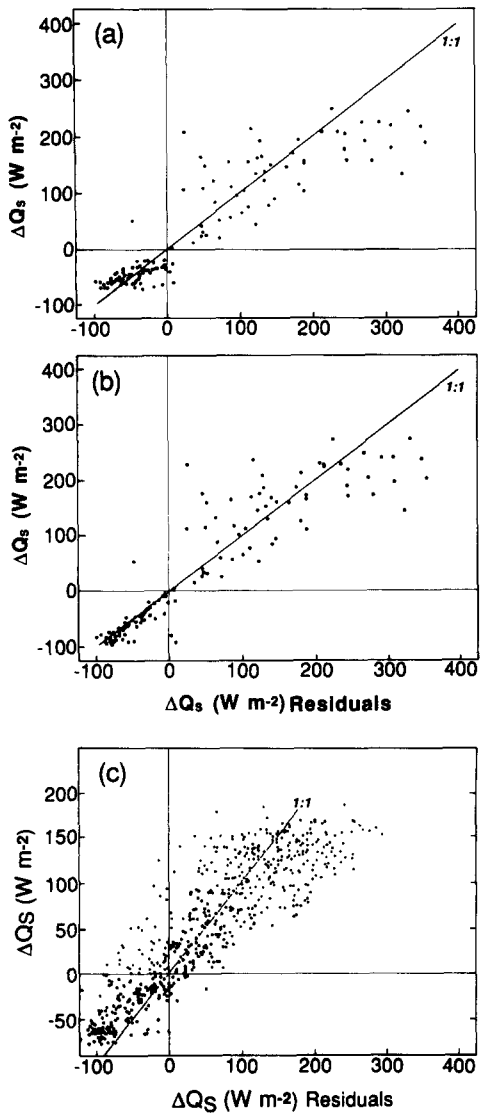

Fig. 3. Storage heat flux residuals vs modeled storage heat flux densities using the objective hysteresis model: (a) all hours equation with changing source area for hours in 1987 when SAM A_{pl} available; (b) $\Delta Q_S = Q^+$ when Q^+ is negative with changing source area for hours in 1987 when SAM A_{pl} available; and (c) all hours equation with static surface description for 1986 data.

Attention is drawn to the fact that the coefficients in the model (Table 1b) are similar to those obtained by Oke and Cleugh (1987). Their coefficients were derived from a multiple regression between measured values of ΔQ_S, Q^*, and $\partial Q^*/\partial t$, whereas those here arise from the objective application of a synthetic concept based on the heating/cooling response of individual surfaces to radiative forcing and the physical nature of the site. Oke and Cleugh's empirical results therefore represent a 'local-scale' integration in contrast to the upward integration of 'micro-scale' effects inherent in the new objective hysteresis approach. The similarity in the coefficients offers indirect support to the present model.

5. COMPARISON WITH OTHER MODELS

5.1. *Comparison between OHM and the simple linear model*

ΔQ_S was calculated for Sunset, Vancouver, using Equation (2) with $a = 0.25$ and $b = -27$ when $Q^* > 0$; and $a = 0.67$ and $b = 0$ when $Q^* < 0$. Table 2b summarizes the statistics for the 1987 comparison between calculated ΔQ_S and 'measured' ΔQ_{SR} values when the error in β was $\leqslant 20\%$. Overall the performance of the OHM is much better than that of the linear model based on measures of goodness of fit, plus the RMSE and MAE are smaller.

The diurnal variation in performance of these two models is illustrated in Figs 4–6. On year day (Y/D) 86/201 the radiant forcing was large with no cloud cover (Fig. 4). OHM shows a reasonable match to measured ΔQ_S values and is an improvement over the linear model. The latter underestimates ΔQ_S in the morning and overestimates in the late afternoon; i.e. the measurements and OHM both depict an out-of-phase relation between Q^* and ΔQ_S which is absent in the linear model. The OHM also comes closer to predicting the maximum value of ΔQ_S, although it is still less than that measured. At night both yield values which are smaller in magnitude than those measured.

The radiant forcing was less on YD 86/243, especially in the morning (Fig. 5), which results in a reduced ΔQ_S. Again the magnitude is better predicted using the OHM, but it is still less than the measured maximum, continuing the evidence of the 'capping' effect noted in section 4.3. Until the peak in ΔQ_S at *ca* 1300 h LAT, the OHM overestimates its size.

The hourly ensemble ΔQ_S for the 1986 data of OHM and the linear model (Fig. 6) shows the increased energy partitioned into ΔQ_S using OHM. In summary, with respect to the measurements OHM truncates the range of ΔQ_S; it mimics the measured hysteresis effect;

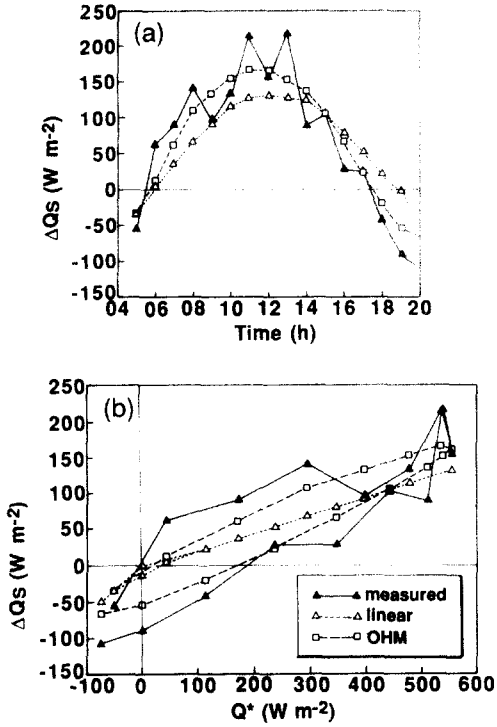

Fig. 4. Measured and modeled storage heat fluxes (the simple linear model and OHM) for Y/D 86/201 at Sunset site, Vancouver, BC: (a) diurnal time series; and (b) relation with net all-wave radiation.

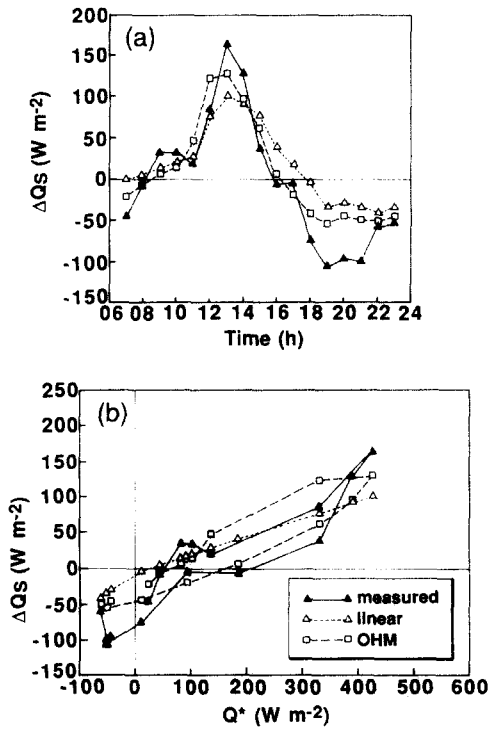

Fig. 5. Same as Fig. 4 but Y/D 86/243.

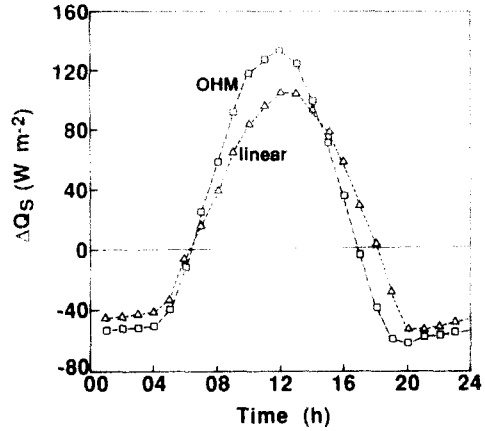

Fig. 6. Ensemble mean of the diurnal cycle of Q^* and ΔQ_S determined from OHM and the simple linear model, for Sunset site, Vancouver.

and is a substantial improvement over the simple linear model.

5.2. *Comparison between OHM and heat content change and weighted plate models*

Two other models have been proposed for the determination of ΔQ_S.

(i) *Heat Content Change Model* (*Peikorz*, 1987; *Kerschgens and Kraus*, 1990). The 'struktur' model of Peikorz (1987) calculates the storage heat flux from the sum of the heat content changes of all components of the urban system:

$$\Delta Q_S = \sum_{i=1}^{n} \Delta Q_{S_i} = \frac{1}{A} \sum_{i=1}^{n} \int_{V_i} C_i \frac{dT}{dt} dV_i, \qquad (6)$$

where C is the heat capacity, T the temperature and V the volume, the subscript i indexes the quantities according to surface type up to n types, A is area and t is time. Evaluation for an urban area requires a large sample of values of C, T and building dimensions.

(ii) *Weighted Plate Model* (*Kerschgens and Hacker*, 1985). The 'versiegelt' model calculates the storage heat flux from the "composite of measured fluxes through two typical surfaces, a paved parking lot and a lawn". The measured fluxes are weighted for the area of greenspace and impervious surfaces:

$$\Delta Q_S = (Q_{G_l} A_l) + (Q_{G_p} A_{im}) \qquad (7)$$

where Q_G is the heat flux measured in the lawn (l) and pavement (p); A is the area. The impervious area (im) is the sum of the building and paved areas.

The data necessary to test these two models are not available for the Sunset site but it is possible to compare OHM with them using information from a field observation programme in Bonn, Germany on 13/14 July 1982 (Kerschgens and Hacker, 1985; Peikorz, 1987; Kerschgens and Kraus, 1990).

The full heat content change model requires information on the orientation of buildings in order to calculate the fractions of sunlit and shaded walls, and

the exterior and interior temperature of the sunlit and shaded building wall and horizontal exterior surfaces. Peikorz (1987) collected the orientation statistics for many buildings, and, depending on wind direction, between 78 and 88 buildings were used to calculate these fractions. The temperature of about 70 points on exterior walls and horizontal surfaces were measured with radiation thermometers (two fixed, one mobile) and the interior wall temperatures of three buildings were monitored with thermographs. The input necessary for OHM (net all-wave radiation, active surface area and surface cover) were also available. The active source areas of the Bonn residential study zone are 45% greenspace, 35% paved and 20% built surfaces. These are based on a 1 km fetch for each of three sectors; viz. 65–90° (13 July 0730 h–14 July 0230 h); 90–130° (14 July 0230 h–14 July 0630 h); and 130–150° (14 July 0730 h–14 July 1730 h). The additional data necessary for the weighted plate model were obtained from profile measurements in a lawn and in a concrete path (Peikorz, 1987).

Comparison of the heat flux densities from the three models for part of two days show reasonable agreement (Fig. 7). There is however a phase shift of about 1 h between OHM and the other two. In the absence of 'measured' heat storage values it is not possible to state which model is closer to the correct value. It might be suspected that the hysteresis model is not properly tuned to the materials of the site but Kerschgens and Kraus (1990) note possible errors in the heat content change model also. Given the simplicity of the input required for OHM and its agreement with both the Sunset measured ΔQ_{SR} and the heat content change approach there seems to be much to commend its use in urban energy balance studies. The weighted plate model follows a similar premise to that of the OHM and is also reasonably easily implemented in the field. Care will have to be exercised in choosing representative surfaces for observation.

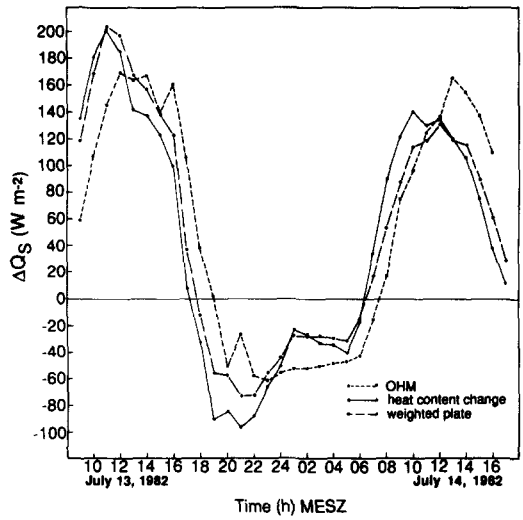

Fig. 7. Storage heat flux for 13 and 14 July 1982 Bonn, Germany calculated using the OHM, weighted plate and heat content change models (MESZ Mitteleuopäische Sommer Zeit—Middle European Summer Time).

6. DISCUSSION

6.1. *The form of the hysteresis equation*

The coefficients resulting from a fit of 'measured' ΔQ_{SR} and Q^* data to a Camuffo and Bernardi (1982) type of equation were determined for different sizes of errors in β for each of three groupings for 1987: all hours; when Q^+ was negative; and when Q^+ was positive. The coefficients obtained when Q^+ is negative are very small suggesting that virtually all the energy for the radiative loss is being removed from storage. The hysteresis term (a_2) is almost negligible. Since there is a bias in the data towards hours when Q^+ is negative, the coefficients for the complete set also are biased towards these hours. Therefore, when hours with only Q^+ positive are fitted as a separate set, the values assigned to a_1 and a_3 are reduced, a_2 is increased, and there is both more scatter (r^2 is smaller) and a larger standard error. Hours with $<10\%$ error in β have a high value of a_1 because Q^+ for these hours is only just greater than zero.

From the foregoing, it appears that the appropriate type of equation to model ΔQ_S should allow for ΔQ_S to be approximately equal to Q^+ when the latter is negative, and when Q^+ is positive the values of the parameters should be similar to those determined when the error in β is between $<12\%$ and $<20\%$ (see Table 3). For some purposes the equality $\Delta Q_S = Q^+$ is inappropriate. For example when calculating nocturnal values of the sensible heat ($Q_{H\beta}$) and latent heat ($Q_{E\beta}$) fluxes from β it results in $Q_{H\beta}$ and $Q_{E\beta}$ equal to zero.

To obtain enough data to study the *monthly* variation in the coefficients of the hysteresis equation it was necessary to use data with $<30\%$ and $<40\%$ error in β (Table 3). This means that the values of individual coefficients are greater. The coefficients for hours when Q^+ is negative are very consistent between months and for most purposes (see earlier discussion)

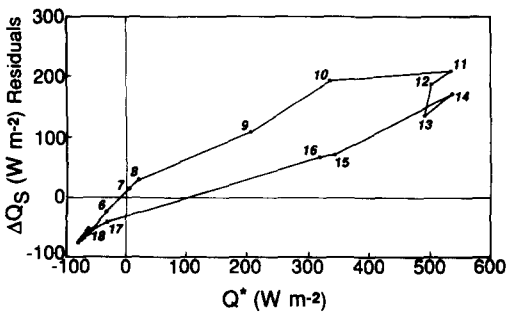

Fig. 8. Plot of hourly ensemble averages of storage heat flux residual and net all-wave radiation for hours when error in Bowen ratio is $<20\%$.

Table 3. Coefficients resulting from a fit of measured 1987 ΔQ_{SR} and Q^* data to the hysteresis model (Camuffo and Bernardi, 1982) for different values of the error in β

% error in β	n	a_1	a_2 (h)	a_3 (W m^{-2})	r^2	$SE^\dagger$ (W m^{-2})
Q^* (positive)						
<10	12	0.96	0.13	−11.8	0.98	5.4
<12	17	0.32	0.19	4.7	0.86	25.2
<13	19	0.37	0.34	−7.9	0.82	35.9
<14	26	0.38	0.58	−29.2	0.79	42.3
<15	30	0.33	0.49	−15.5	0.71	46.4
<16	40	0.33	0.51	−16.8	0.62	59.7
<17	47	0.35	0.51	−20.8	0.66	60.3
<18	56	0.35	0.46	−16.5	0.65	59.3
<20	72	0.37	0.43	−14.4	0.62	64.1
<25	115	0.42	0.52	−30.5	0.66	63.3
<30	168	0.45	0.43	−32.5	0.63	67.0
<40	246	0.46	0.37	−30.8	0.64	65.9

† SE—standard error of ΔQ_S.

Table 4. Percentages of surface cover type in the Sunset study area for use with the objective hysteresis model. Total area = 2D greenspace + 3D buildings (roof + walls) + 2D impervious

	Surface cover type (%)			
		Buildings		
	Greenspace	Roof	Wall	Impervious
2 km radius Circle				
Cleugh (1990)	43	13	33	11
Grimmond (1988)	31	23	26	20
Quadrant NE	28	24	28	20
SE	27	25	27	21
SW	32	21	24	23
NW	36	21	25	18
A_{pl}				
Mean (n = 1715)	30	23	27	20
Sd	5	2	2	2
Max	66	27	30	34
Min	23	9	10	14
Error in $\beta \leqslant 20\%$				
All hours: mean	31	23	27	20
Q^+ positive:mean	31	23	28	20
A_{sc}				
Mean (n = 3779)	32	22	26	20
Sd	6	2	3	2
Max	52	26	30	25
Min	24	16	19	14
Error in $\beta \leqslant 20\%$				
All hours: mean	32	22	25	20
Q^+ positive:mean	29	23	28	20
Mean when applied to hours when Q^+ is positive				
A_{pl} and A_{sc}	30	23	27	20

ΔQ_S could be set equal to Q^+ under all conditions. A plot of the ensemble averages of ΔQ_S and Q^* shows that the hysteresis pattern reported by Oke and Cleugh (1987) in urban areas during summer also occurs in winter and spring (Fig. 8).

The coefficients for the hours when Q^+ is positive are more variable. For the January–February period (Y/D 87/21–59) there are too few data to be useful. The a_1 coefficients for April (91–120) and June (152–179) are larger than for the other months. However, it is reasonable to conclude there is no clear trend towards a greater percentage of Q^+ going into ΔQ_S at this site as the seasons proceed from winter to summer.

6.2. *Influence of surface cover description*

In this section the influence and merits of using a static or dynamic surface description in the objective hysteresis model are discussed. Table 4 gives the

surface cover proportions calculated according to the static (2 km radius) and dynamic (A_{pl} and A_{se}) description approaches (section 3.1). The latter two are expressed as means, standard deviations and ranges.

When using the database, the static proportions of the surface cover present in the 2 km radius circle are very similar to the mean when the dynamic source areas are taken into account. The maximum percentage difference between the mean of the various techniques is 2% for any particular surface cover type. The maximum variability occurs for the greenspace, with a range of approximately 40% (A_{pl}). The range of the other three surface types is approximately 20% (A_{pl}). The maximum and minimum values of the coefficients of the surfaces used in the hysteresis model are associated with the extremes in cover types, as would be expected (see Table 4). The a_1 and a_3 coefficients are similar for greenspace, roofs, and canyon. The a_2 are similar for greenspace, roofs and impervious surface types. The maximum (0.41) and minimum (0.36) values of a_1 occur when the pavement proportion is at its maximum and minimum, respectively. The maximum a_2(0.33) and the minimum absolute value of a_3(26.9) are associated with the maximum vegetation and minimum wall area, respectively. The minimum a_2(0.25) is associated with the maximum wall area. The maximum absolute value of a_3(32.1) occurs when the pavement area is at its maximum.

OHM is conservative with respect to changes in proportions of surfaces present. Table 1c presents the

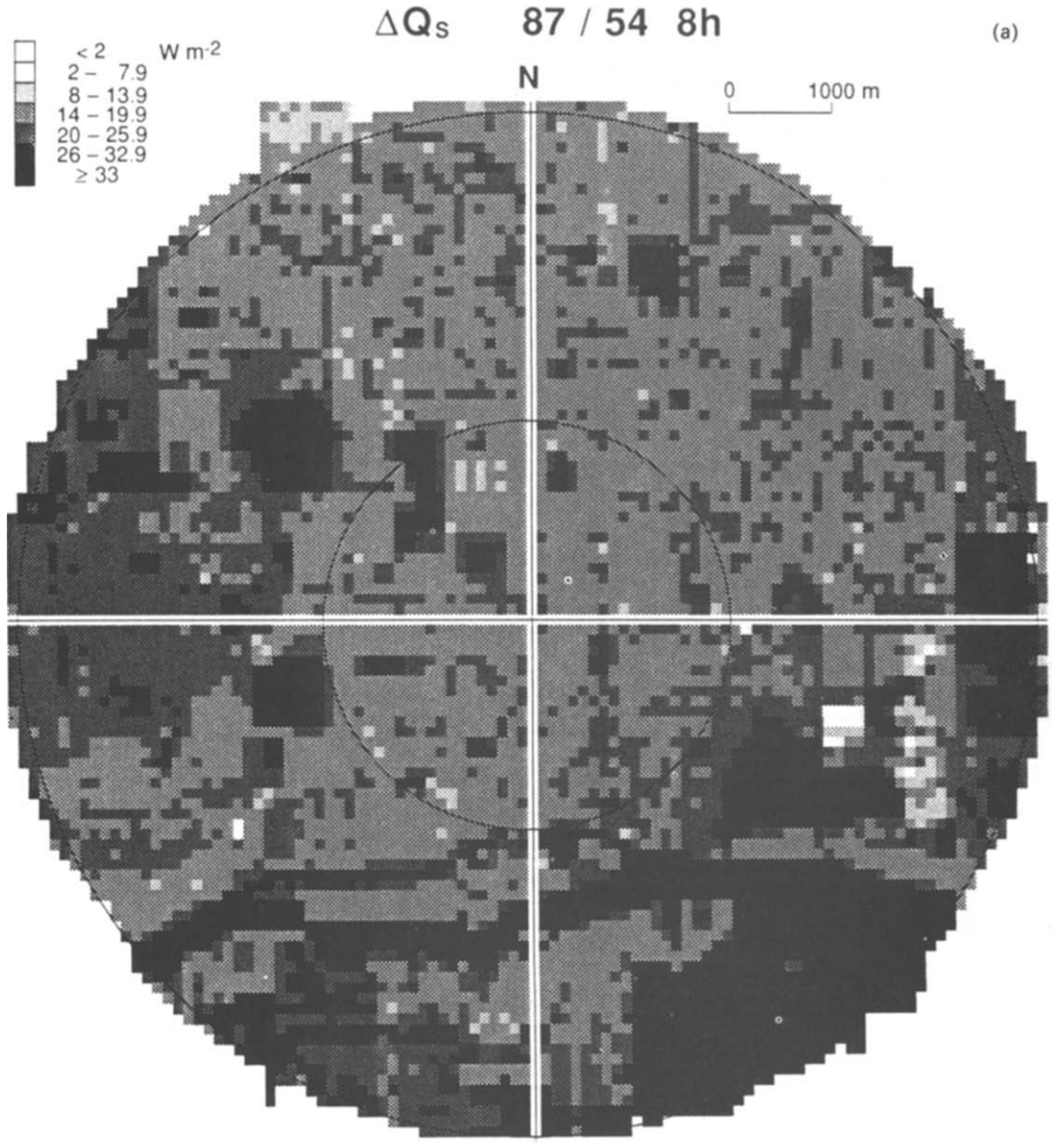

Fig. 9(a).

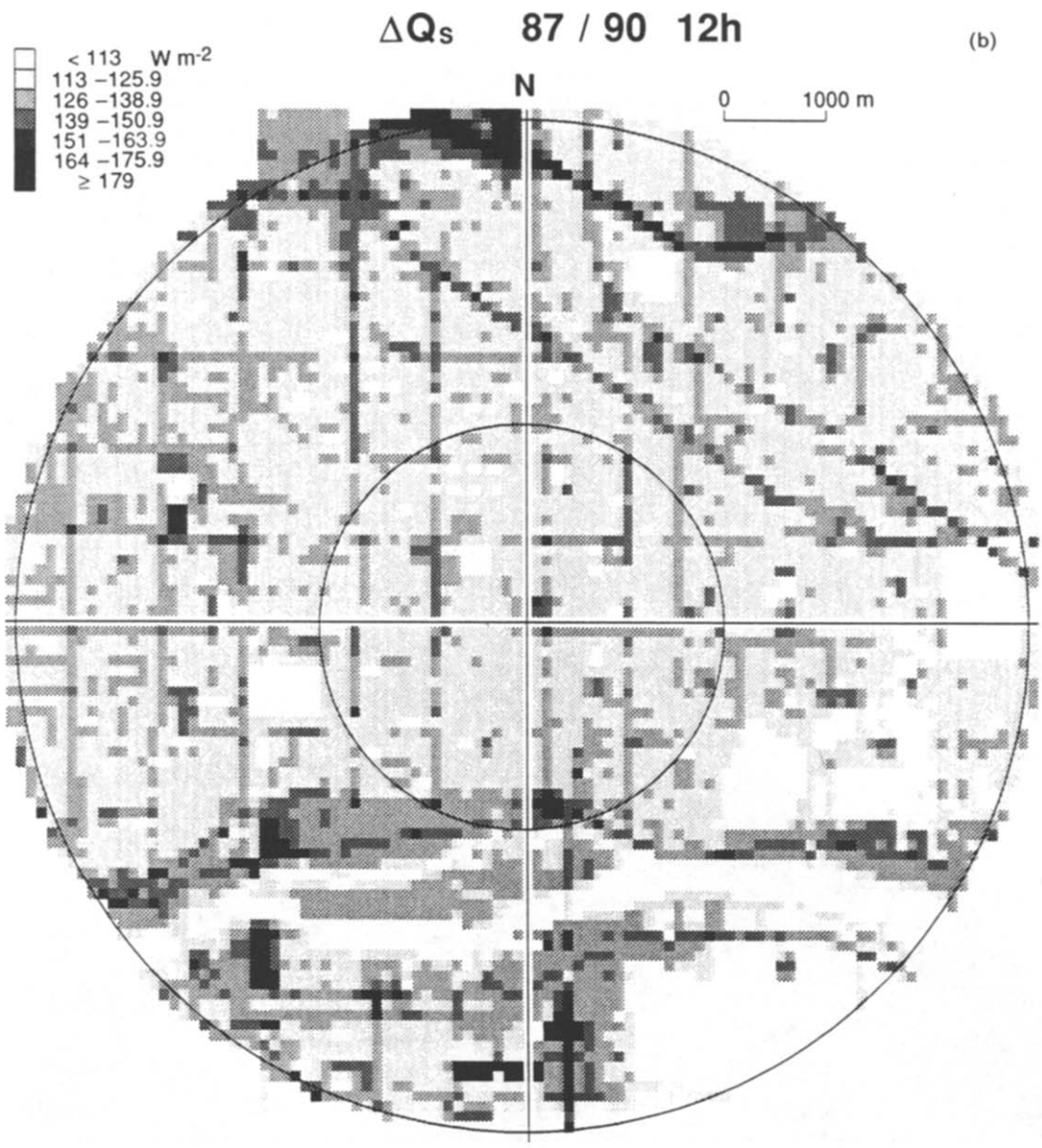

Fig. 9. Map of storage heat flux for Vancouver, BC centered on measurement tower described in text: (a) 0800 h LAT Y/D 87/54; and (b) 1200 h LAT Y/D 87/90.

mean equations when the turbulent source areas are used to determine the surface proportions for the model. The equations vary very little, and as already noted, the ranges are also not very large when the varying source areas are taken into account. The mean equations for the source areas and the equation for the fixed 2 km radius circle are virtually the same. The coefficients are very similar to those determined as the best fit when Q^+ is positive and β has an error of 12–20%. When the surface is described by the mean for the 2 km circle (surface database) or is allowed to vary due to dynamic changes in source area there is some variability but on the whole there is very close agreement between the modeled fluxes. The variation is probably smaller than the deviation from the 'true' ΔQ_S. Therefore, if one is not interested in hour-to-hour variability the use of a mean surface description is satisfactory in an area of reasonably uniform land-use and building density.

Using the urban surface database it is possible to calculate the size of the storage heat flux density for each grid square for any hour or any energy conditions. Figures 9a and 9b are maps of ΔQ_S when the error in $\beta < 20\%$ for Y/D 87/54 0800 h LAT ($Q^+ = 41$ W m^{-2}, $\partial Q^+/\partial t = 127$ W m^{-2} h^{-1}) and Y/D 87/90 1200 h LAT ($Q^+ = 426$ W m^{-2}, $\partial Q^+/\partial t = -28$ W m^{-2} h^{-1}), respectively and Figs 10a and 10b are maps of the vegetated and paved areas at this site. ΔQ_S ranged from -4 W m^{-2} to 39 W m^{-2} at 0800 h LAT and from 100 to 189 W m^{-2} at 1200 h LAT. The parks

have the highest ΔQ_S (compare Fig. 9a with Fig. 10a) at 0800 h LAT. At midday the road pattern is evident (compare Fig. 9b with Fig. 10b). The grid squares which have the largest flux are not the same at both times, although those with the smallest fluxes are similar. This indicates that consideration of the source area for some sites may be more critical than would appear to be the case at the present study site. Changing the surface types influences the calculated ΔQ_S in a different manner through the day because of the changing weighting of the a_1 and a_2 coefficients.

Inspection of the coefficients for each surface type in Table 1a reveals an almost surprisingly similar magnitude of the very important a_1 values which set the overall partitioning into storage. As a result the weighted final value for the Sunset suburban area is also similar. This lack of marked difference in the coefficients will lead to a reduction in the storage variability resulting from differences in active area and surface cover and means that the scheme is relatively conservative. It may also help to explain the results of Kerschgens and Kraus (1990) who show that measurements of substrate heat flux into horizontal grass and impervious surfaces weighted by the areal fraction of surface covered by such surfaces give storage values almost in agreement with a very much more complex scheme. Clearly there is a great need for more studies of the relation between ΔQ_S and Q^* in urban materials such as various types of roofing, glass, stone, wood, etc., and more careful studies of ΔQ_S from energy balance or heat content change at a variety of urban sites. The rather large variability of coefficients from

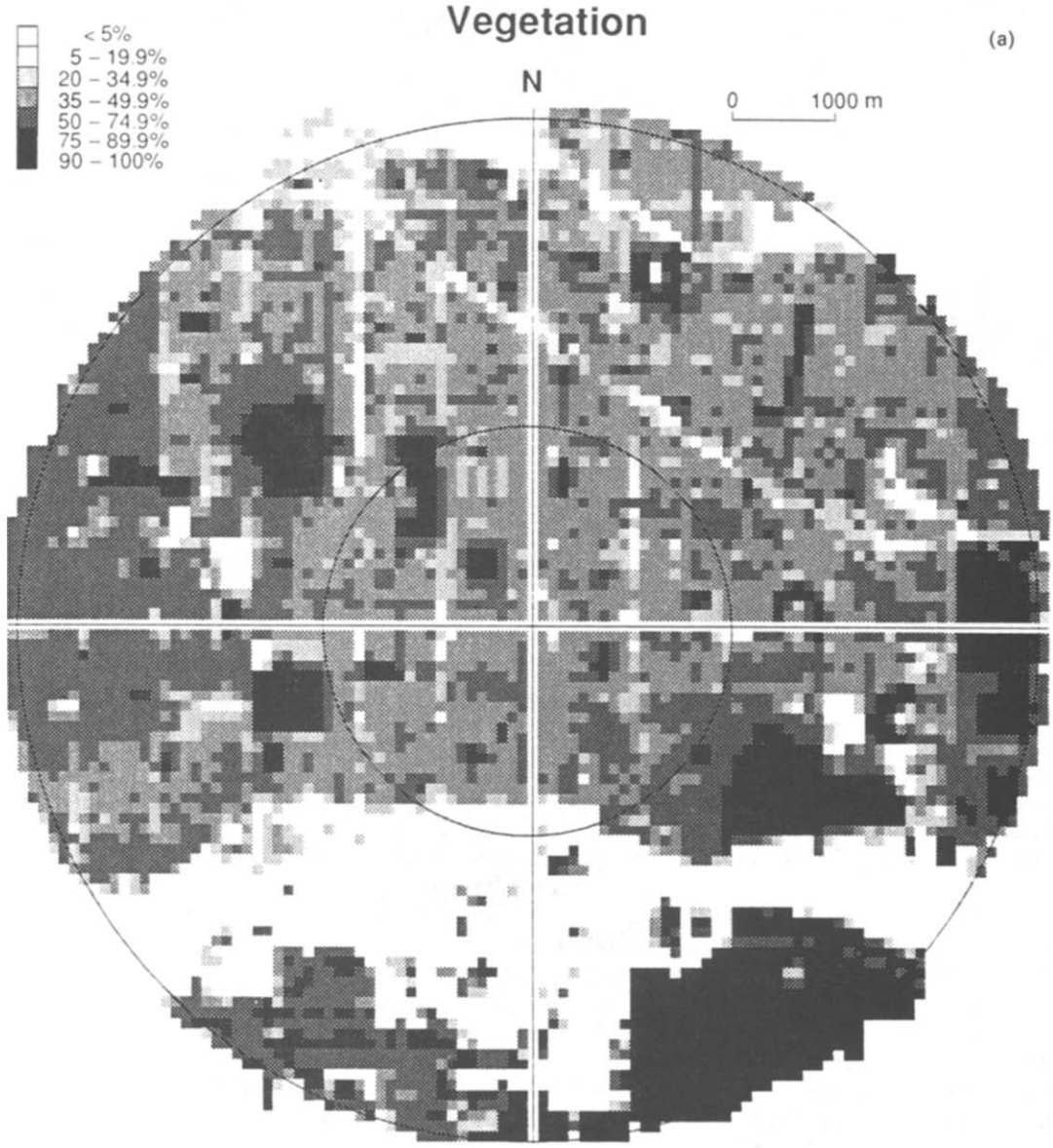

Fig. 10(a).

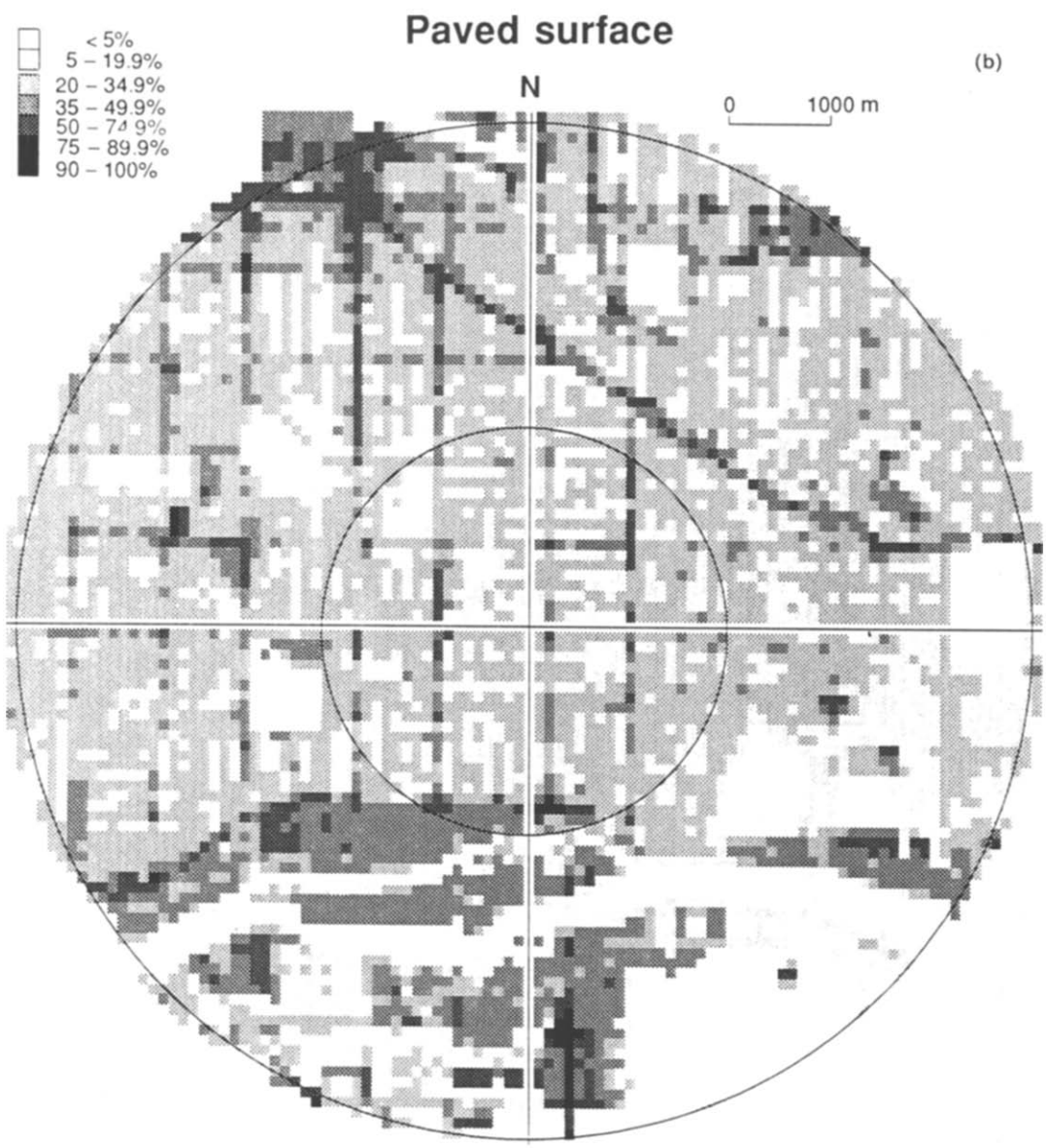

Fig. 10. Map of surface types for same area as Fig. 9: (a) total vegetation; and (b) paved area.

such surfaces is a weakness in the OHM approach that should be addressed. Only then will the true magnitude and potential importance of intra-urban variation, and urban–rural differences, of heat storage be known.

6.3. *Annual storage heat flux*

It is relevant to enquire whether the form of the hysteresis model makes sense in relation to the annual storage input/output regime. This was considered using hourly net all-wave radiation for a complete year collected at a suburban site (Kerrisdale) 8 km to the west of the Sunset site. Table 5 shows that when these data are input to the objective hysteresis model (with separate equations for daytime and nighttime) at Kerrisdale there are 5 months of net storage heat loss; March and October are the transition months between net gain and net loss; and the peak gain occurs in June. It is calculated that in 1982 there was a small net gain in ΔQ_S on an annual basis. Ideally there should be almost zero net heat storage over the annual period, but the result is considered satisfactory.

7. CONCLUSIONS

(1) Theoretical and empirical evidence indicate that it is necessary to include non-linear (hysteresis) effects into schemes to estimate urban heat storage.

(2) A test of an objective hysteresis model, which requires only net all-wave radiation and surface cover information, using an extensive set of energy balance

Table 5. Mean daily Q^* and ΔQ_s by month for Kerrisdale, Vancouver 1982

	Q^* (W m^{-2})	Q_F† (W m^{-2})	ΔQ_s (W m^{-2})
1982			
YD 22–31 + ‡	−0.7	9.4	−18.9
31–59	20.2	9.1	−12.2
60–90	54.2	8.9	0.9
91–120	102.9	8.3	18.1
121–151	134.1	7.7	28.7
152–181	144.3	7.6	32.7
182–212	123.6	7.6	26.2
213–243	103.6	7.7	17.7
244–273	66.6	8.3	4.4
274–304	30.6	8.9	− 5.2
305–334	3.7	9.1	−18.2
335–365	−7.3	9.4	−20.2
Year	64.9	8.5	4.6

† Q_F mean values from 1987 data. Assuming that the flux is similar for the two areas and years; and that the flux is symmetrical in the year around June.

‡ The January period was measured in two parts: Y/D 82/22–31 and 83/1–21.

data and detailed site inventory, confirms its ability to simulate most of the essential features of the heat storage regime of a suburban area. The diurnal performance shows that OHM successfully captures the general magnitude and pattern of the diurnal heat storage regime. Therefore it is generally appropriate for hourly estimates of heat storage at the scale of land-use zones. There is evidence that the OHM underestimates values at the peak of the daily input cycle and the output just after sunset; and its phase may be delayed by about 1 h.

(3) The model has been tested with equal success in both winter and summer. Also it can be used for modeling the annual cycle.

(4) The parameterization is relatively insensitive to the characteristics of the surface cover. Therefore, the use of the source area scheme is probably only warranted in areas of great spatial inhomogeneity. It is possible that intra-urban variation of heat storage is relatively conservative.

(5) The weighted plate method shows close similarity to the heat content change method but has the advantage of not requiring the intensive temperature measurements. It also lends support to the objective hysteresis approach of calculating the storage flux by taking into account the proportions of different surfaces present.

(6) There is a need for more research on this topic including the thermal storage response of individual surface materials, whole buildings and other structures such as canyons. It is also necessary to obtain estimates of heat storage in other urban areas with very different surface character (e.g. small greenspace, densely packed buildings and buildings with large thermal mass) and at other times of the year.

Other issues that need to be addressed include: firstly, the response of the model as Q^* goes negative at the end of the day. Empirical evidence suggests there is a large release of ΔQ_S in the late afternoon but OHM does not incorporate this feature. This may be due to the lack of consideration of the temporal influence of vertical surfaces oriented in different directions in the model. It is also important to verify the small a_2 values used for canyons. Given that one-third of the active area is associated with this surface it plays a major role in damping the hysteresis effect. Secondly, there is no incorporation of the influence of wind on ΔQ_S. In areas where wind is an important control on the partitioning of energy the current model which only includes Q^* as a control would not predict its effects on the changes in energy partitioning. One way to include this would be to model ΔQ_S as a function of Q_H. The problem associated with this is that Q_H is not routinely available. Thirdly, Roth (1991) raises the possibility that the 'capping' effect may be an error in ΔQ_{SR} rather than a flaw in OHM. He notes that due to dissimilarity in the diffusion coefficients for heat and water vapor and sampling problems, values of β measured using wet- and dry-bulb gradients are overestimated in the afternoon at this site and at this height. This implies that some of the large ΔQ_{SR} values are overestimated and no 'capping' effect is present.

Acknowledgements—Special thanks are due to Dr M. J. Kerschgens for providing the ancillary data from the G. Peikorz Diploma study; and Drs H. P. Schmid and C. J. Souch who helped in the field and for useful discussion. This research was supported by grants to T.O. from the Natural Sciences and Engineering Research Council of Canada and the Atmospheric Environment Service of Environment Canada. We are grateful to Scott Ferguson who analysed the canyon data set. The field site was made available by BC Hydro and Power Authority.

REFERENCES

Aston A. R. (1985) Heat storage in a young Eucalpyt forest. *Agr. For. Met.* **35**, 281–297.

Bach W. (1970) An urban circulation model. *Arch. Met. Geoph. Biokl. Ser B.* **18**, 155–168.

Camuffo D. and Bernardi A. (1982) An observational study of heat fluxes and the relationship with net radiation. *Boundary-Layer Met.* **23**, 359–368.

Clarke R. H., Dyer A. J., Brook P. R., Reid D. G. and Troup A. J. (1971) The Wangara Experiment—Boundary Layer Data, No. 19, Division of Meteorological Physics, C.S.I.R.O., Australia.

Cleugh H. A. (1990) Development and evaluation of suburban evaporation model: a study of surface and atmospheric controls on the suburban evaporation regime. Ph.D. Thesis, The University of British Columbia, Vancouver.

Clothier B. E., Clawson K. L., Pinter P. J., Jr, Moran M. S., Reginato R. J. and Jackson R. D. (1986) Estimation of soil heat flux from net radiation during the growth of alfalfa. *Boundary-Layer Met.* **37**, 319–329.

de Bruin H. A. R. and Holtslag A. A. M. (1982) A simple parameterisation of sensible and latent heat during daytime compared with the Penman-Monteith concept. *J. appl. Met.* **21**, 1610–1621.

Doll D., Ching J. K. S. and Kaneshiro J. (1985) Parameterisation of subsurface heating for soil and concrete using net radiation data. *Boundary-Layer Met.* **32**, 351–372.

Fuchs M. and Hadas A. (1972) The heat flux density in a non-homogeneous bare loessial soil. *Boundary-Layer Met.* **3**, 191–200.

Goward S. N. (1981) Thermal behavior of urban landscapes and the urban heat island. *Phys. Geog.* **2**, 19–33.

Grimmond C. S. B. (1988) An evapotranspiration-interception model for urban areas. Ph.D. Thesis. The University of British Columbia, Vancouver.

Grimmond C. S. B. (1992) Seasonal nature of the urban energy balance. *Int. J. Clim.* (in press).

Grimmond C. S. B., Oke T. R. and Steyn D. G. (1986) Urban water balance I: A model for daily totals. *Wat. Resour. Res.* **22**, 1397–1403.

Idso S. B., Aase J. K. and Jackson R. D. (1975) Net radiation-soil heat flux relations as influenced by soil water content variations. *Boundary-Layer Met.* **9**, 113–122.

Kerschgens M. J. and Drauschke R. L. (1986) On the energy budget of a wintry mid-latitude city atmosphere. *Contrib. Atmos. Phys.* **59**, 115–125.

Kerschgens M. J. and Hacker J. M. (1985) On the energy budget of the convective bounday layer over an urban and rural environment. *Contrib. Atmos. Phys.* **58**, 171–185.

Kerschgens M. J. and Kraus H. (1990) On the energetics of the urban canopy layer. *Atmospheric Environment* **24B**, 321–328.

Lettau H. H. (1951) Theory of surface temperature and heat transfer oscillations near a level ground surface. *Trans. Am. geophys. Union* **32**, 189–200.

Mark D. M. and Church M. (1977) On the misuse of regression in earth science. *Math. Geol.* **9**, 63–75.

McCaughey J. H. (1985) Energy balance storage terms in a mature mixed forest at Petawawa Ontario – a case study. *Boundary-Layer Met.* **31**, 89–101.

McCaughey J. H., Mullins D. W. and Publicover M. (1987) Comparative performance of two reversing Bowen Ratio measurement systems. *J. Atmos. Oceanic Technol.* **4**, 724–730.

Monteith J. L. (1973) *Principles of Environmental Physics*. Edward Arnold, London.

Moore C. J. and Fisch G. (1986) Estimating heat storage in Amazonian tropical forest. *Agr. For. Met.* **38**, 147–169.

Narita K., Sekine I. and Tokuoka I. (1984) Thermal properties of urban surface materials – study on heat balance at asphalt pavement. *Geog. Rev. Japan* **57A**, 639–651.

Nash J. E. and Sutcliffe J. V. (1970) River flow forecasting through conceptual models. Part I – a discussion of principles. *J. Hydrol.* **10**, 282–290.

Novak M. D. (1981) The moisture and thermal regimes of a bare soil in the Lower Fraser Valley during spring. Ph.D. Thesis, The University of British Columbia, Vancouver.

Nunez M. (1974) The energy balance of an urban canyon. Ph.D. Thesis, The University of British Columbia, Vancouver.

Oke T. R. and Cleugh H. A. (1987) Urban heat storage derived as energy budget residuals. *Boundary-Layer Met.* **39**, 233–245.

Oke T. R., Kalanda B. D. and Steyn D. G. (1981) Parameterisation of heat storage in urban areas. *Urban Ecol.* **5**, 45–54.

Peikorz G. (1987) Die energiebilanz einer stadtischen struktur. Dipl. Meteorologie. Rheinische Friedrich-Wilhelm-Universitat, Bonn.

Roth M. (1991) Turbulent transfer characteristics over a suburban surface. Ph.D. Thesis. The University of British Columbia, Vancouver.

Schmid H. P. and Oke T. R. (1990) A model to estimate the source area contributing to surface layer turbulence at a point over a patchy surface. *Q. Jl R. met. Soc.* **116**, 965–988.

Schmid H. P., Cleugh H. A., Grimmond C. S. B. and Oke T. R. (1991) Spatial variability of energy fluxes in suburban terrain. *Boundary-Layer Met.* **54**, 249–276.

Sellers W. D. (1965) *Physical Climatology*. University of Chicago Press, Chicago.

Taesler R. (1980) Studies of the development and thermal structure of the urban boundary layer in Uppsala, Part I: Experimental Program; and Part II: Data, analysis and results, Report 61, Met. Instit., Uppsala Univ., Uppsala.

Wilmott C. J. and Wicks D. E. (1980) An empirical method for the spatial interpolation of monthly precipitation within California. *Phys. Geog.* **1**, 59–73.

Yap D. H. (1973) Sensible heat fluxes in and near Vancouver, BC. Ph.D. Thesis, The University of British Columbia, Vancouver.